Voltage-Induced Switching of Nanoscale Magnetic Tunnel Junctions

J. G. Alzate[1*], P. Khalili Amiri[1**], P. Upadhyaya[1], S.S. Cherepov[1], J. Zhu[2], M. Lewis[1], R. Dorrance[1], J. A. Katine[3], J. Langer[4], K. Galatsis[1], D. Markovic[1], I. Krivorotov[2], and K. L. Wang[1***]

[1] Department of Electrical Engineering, University of California, Los Angeles, CA 90095, USA
[2] Department of Physics and Astronomy, University of California, Irvine, CA 92697, USA
[3] Hitachi Global Storage Technologies, San Jose, CA 95135, USA
[4] Singulus Technologies, Kahl am Main, Germany
Email: * jalzate@ucla.edu, ** pedramk@ucla.edu, *** wang@ee.ucla.edu

Abstract

We demonstrate voltage-induced (non-STT) switching of nanoscale, high resistance voltage-controlled magnetic tunnel junctions (VMTJs) with pulses down to 10 ns. We show ~10x reduction in switching energies (compared to STT) with leakage currents < 10^5 A/cm^2. Switching dynamics, from quasi-static to the nanosecond regime, are studied in detail. Finally, a strategy for eliminating the need for external magnetic-fields, where switching is performed by set/reset voltages of different amplitudes but same polarity, is proposed and verified experimentally.

Introduction

Magnetic tunnel junctions (MTJs) have emerged as the building blocks of spintronic circuits due to their large tunneling magnetoresistance (TMR) ratios, and the possibility of integration with conventional semiconductor electronics. The use of spin-polarized currents to switch magnetization in MTJs, e.g., via spin-transfer-torque (STT), however, limits the energy efficiency and density of STT-based MRAM, due to Ohmic losses and the need for large transistors to drive the required switching current, respectively (1). Therefore, electric-field control of magnetism could result not only in a magnetoelectric random access memory (MeRAM) with improved energy efficiency and density compared to STT-RAM, but also in new applications for nonvolatile spintronic devices, by making them energetically competitive compared to traditional semiconductor solutions for logic and computation.

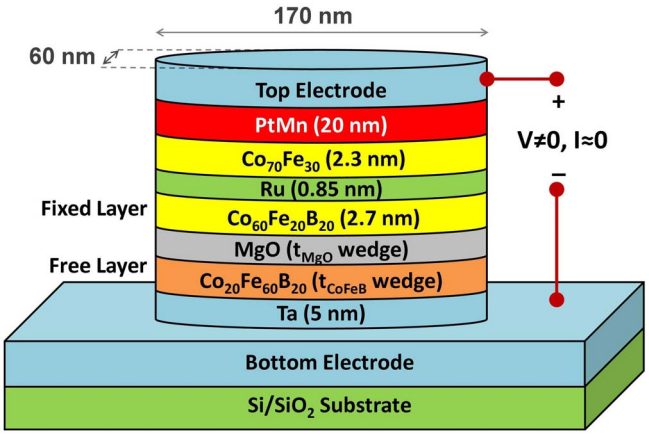

Fig. 1 The devices used in this work were 170 nm × 60 nm elliptical magnetic tunnel junctions, with high resistance (thick MgO) designed to reduce the effect of current-induced torques. We obtained qualitatively similar results on devices with different dimensions patterned on the same wafer. Voltages were applied across the MgO to induce a change of the interfacial anisotropy in the CoFeB free layer, and the state of the magnetic bit was read out via the TMR effect.

In this work, we demonstrate voltage-induced switching of 170 nm × 60 nm VMTJs (see Fig. 1) by exploiting the voltage-controlled magnetic anisotropy (VCMA) (2)-(6) at the interface between the Fe-rich CoFeB free layer and MgO. This interfacial effect is of considerable practical value, given that it uses materials widely adopted by MRAM technology. In fact, VMTJs for MeRAM could be fabricated in the back-end-of-line process steps (BEOL) of CMOS technology (see Fig. 2), similar to STT-RAM technology.

In our devices, the free layer thickness is chosen such that the interfacial (voltage-controlled) perpendicular anisotropy is close to compensating the easy-plane shape anisotropy (7), a condition that enhances the tunability of the coercivity by voltage. In particular, Fig. 3 demonstrates that the coercivity can be reduced from ~ 120 Oe at equilibrium to ~ 10-20 Oe by applying voltages ~ 1 V due to the VCMA effect.

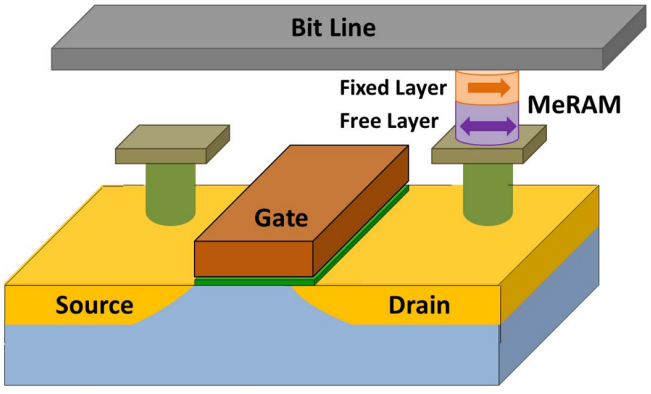

Fig. 2 Illustration of a 1-transistor/1-VMTJ MeRAM cell. Writing is performed by setting the source line and word line (source and gate contacts) to low and high voltages, respectively, and applying the set/reset voltage to the bit line.

VCMA-Induced Switching

The reduction of the coercivity due to the VCMA effect is exploited to switch the magnetization of the free layer of our VMTJs without the influence of spin-polarized currents. To illustrate the switching process, consider a VMTJ resting in the high-resistance state (point A in Figs. 4 and 5). Note that the magnetization has an out-of-plane component due to the competition between anisotropies described before. This competition results in a non-trivial dependence of coercivity on the applied voltage and the interfacial anisotropy. When a positive voltage pulse is applied, the perpendicular anisotropy of the free layer decreases, reducing its coercivity. As a result, under the new energy landscape the magnetization is forced to thermally relax to the low-resistance intermediate state (point B) due to the effective magnetic field H_{eff} acting on the free layer. After the voltage is removed, the magnetization reconfigures into the opposite direction (point C), completing the reversal process. Figures 4 and 5 show that the sign of the overall effective magnetic field determines the direction of switching, and hence the voltage-induced switching is unidirectional for a given H_{eff}.

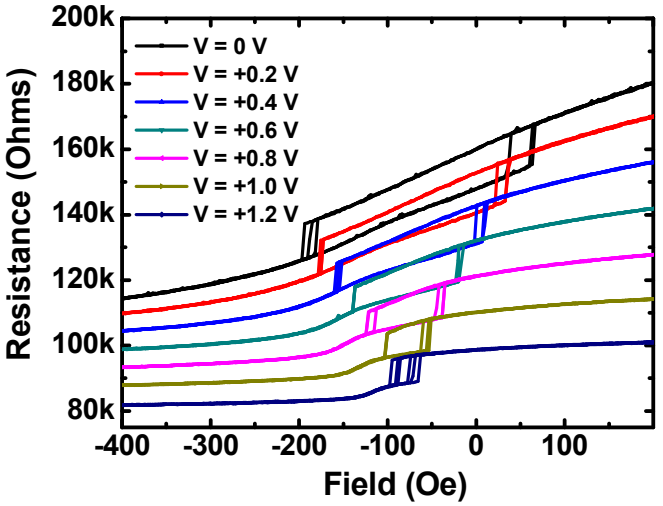

Fig. 3 The resistance versus in-plane magnetic field measurements (along the main axis of the nanopillar) demonstrate voltage-dependent coercivity and TMR ratio. For our devices, positive voltages decrease the interfacial perpendicular anisotropy (VCMA), consistent with previous studies (2)-(6), and result in a reduction of the coercivity due to a non-trivial dependence of coercivity on anisotropy near the compensation thickness, which was also reproduced in micromagnetic simulations. Given the thick MgO in our samples, the change in coercivity is purely due to voltage effects.

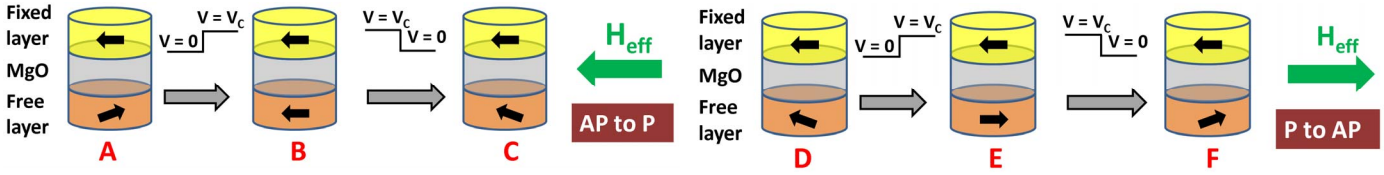

Fig. 4 The initial equilibrium state (A, D) shows an out-of-plane component due to the compensation between in-plane shape anisotropy and out-of-plane interfacial anisotropy, considering the contribution from second order term. When a positive voltage $V = V_C$ is applied, the reduction of the perpendicular anisotropy results in a meta-stable, in-plane state (B, E), which is defined by the direction of the effective magnetic field H_{eff} in the free layer. Once the voltage is released, the state is relaxed to the final equilibrium state (C, F).

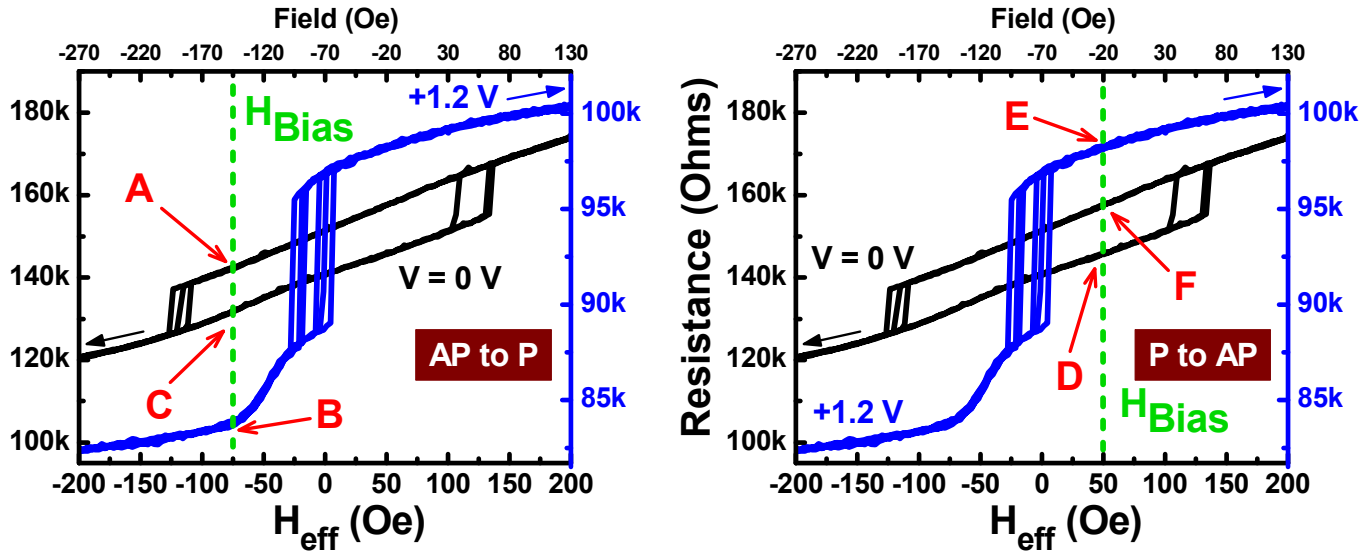

Fig. 5 The effective magnetic field H_{eff} (bottom horizontal axis) is defined as $H_{eff} = H_{Bias} - H_{off}$, where H_{Bias} (top horizontal axis) is the externally applied magnetic field during measurement, and H_{off} is the non-zero offset field due to the coupling of free and fixed layers in the device. Once the voltage is applied, the initial state (A, D) is forced to the only available state (B, D). When the voltage is released, switching in a given direction is obtained depending on the sign of H_{eff} (C,F).

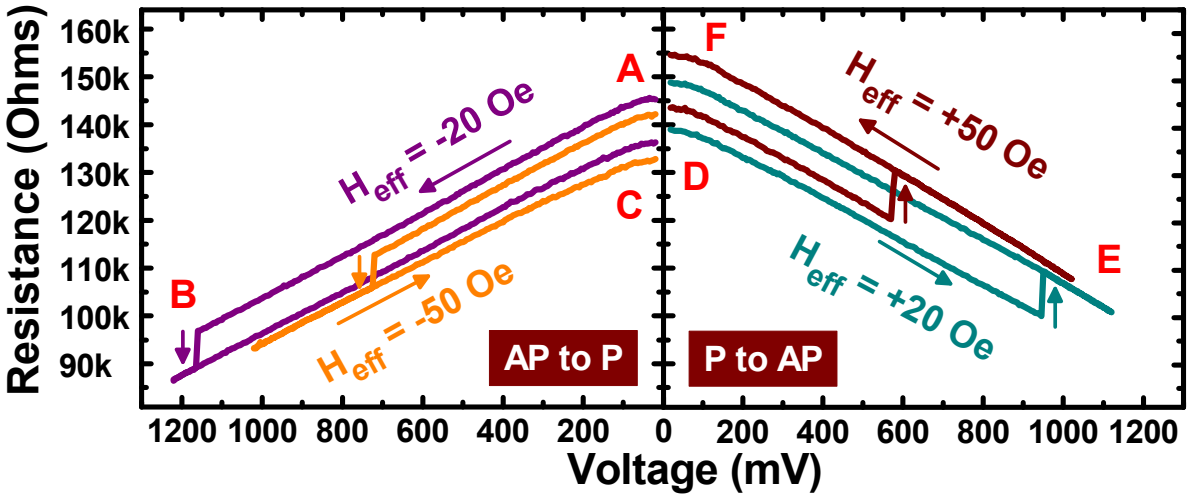

Fig. 6 Quasi-static resistance versus voltage curves for different effective magnetic fields H_{eff}. Resistance is measured while the bias voltage is applied, therefore the voltage-dependence of the VMTJ resistance is observed. The loops demonstrate switching for H_{eff} as small as ± 20 Oe. Note that switching in both directions is performed with voltages of the same polarity.

Switching Dynamics

The voltage-driven switching hysteresis of our devices can be observed in the measured quasi-static loops shown in Fig. 6. The observed voltage dependence of VMTJ resistance for both P and AP states is assumed to be due to a combination of the change of the canted state of the free layer due to the applied voltage, as well as the bias dependence of TMR.

Note that switching in both directions was performed using voltages of the same polarity, with a small bias magnetic field to determine the direction. In the quasi-static regime, the devices can be switched with effective magnetic fields as small as ± 20 Oe when a voltage of ~1 V is applied to them. The large resistance of our VMTJ (resistance-area *RA* product ~ 1300 Ω-μm^2) assured that the leakage currents were always small ($I_{leakage}$ < 10 μA), and therefore the observed phenomena correspond to purely voltage-controlled effects. By increasing the thickness of the MgO tunneling barrier (i.e., increasing the resistance of the VMTJ), the leakage current can be decreased even further without affecting the VCMA-driven switching mechanism.

We next performed pulsed switching experiments on the devices. Fig. 7 shows the dependence of the mean switching voltage V_c as a function of the applied voltage pulse width t, measured down to 10 ns. The switching voltage is found to fit well to a thermal activation model of the form

$$V_C = V_{C0}(1 - \Delta^{-1}\ln(t/\tau_0)) \qquad (1)$$

where $\tau_0 \sim 1$ ns is the attempt time, V_{C0} corresponds to the switching voltage at $t = \tau_0$, and Δ is proportional to the energy barrier that the magnetization traverses during the reversal process, which is generally smaller than the equilibrium energy barrier due to the applied switching voltage.

The results demonstrate voltage-induced switching of the free layer with amplitudes of ~1 V for both low (parallel, or P) to high (anti-parallel, or AP), and AP to P switching directions, translating into switching energies (with C being the capacitance of the VMTJ)

$$E = I_{leakage}^2 Rt + CV_C^2 \qquad (2)$$

of ~60 fJ (at $t = 10$ ns) for our experiment, one order of magnitude smaller than comparable purely STT-based devices. The switching energy can be reduced below 1 fJ by further decreasing the leakage current and/or decreasing the switching pulse duration.

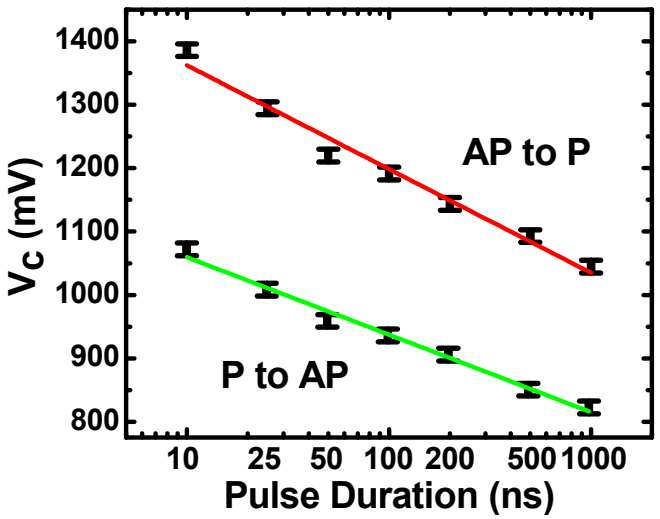

Fig. 7 Switching voltage as a function of write time for different switching directions. Switching at 10 ns is ~10 times more energy-efficient than in comparable STT-RAM memory bits. Different switching directions were realized through small external magnetic fields (H_{eff} = +80 Oe and −80 Oe, respectively).

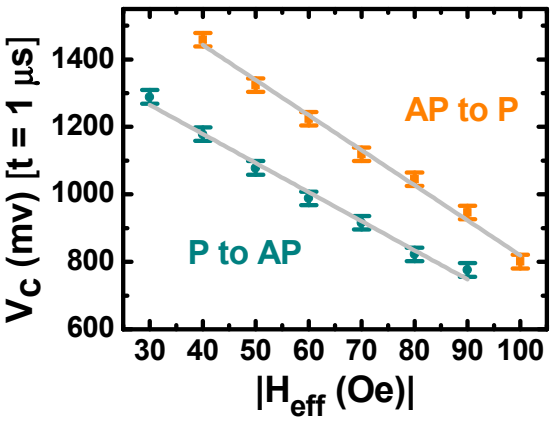

Fig. 8 A linear reduction of the required switching voltage (measured using pulses with t = 1 µs) for both directions is observed as H_{eff} increases.

We also measured the dependence of the switching voltage on the effective magnetic field H_{eff}. Figure 8 confirms the expected decrease of the switching voltage with increasing H_{eff}, indicating a trade-off between the switching voltage amplitude and the in-plane magnetic field which assists the switching process.

Finally, we characterized the thermal stability of our VMTJ in its equilibrium state. This was performed by measuring the mean time for thermally-activated switching for different magnetic fields applied to the device, as shown in Fig. 9. Extrapolation of the curve to the standby (H_{eff} = 0 Oe) condition yields a retention time of ~1.7 × 10^9 seconds (> 50 years), sufficient stability for nonvolatile memory operation.

Combined VCMA + STT Switching

To overcome the need for external magnetic fields that assist the switching process and determine the direction of the reversal, we propose to utilize a small non-zero leakage current

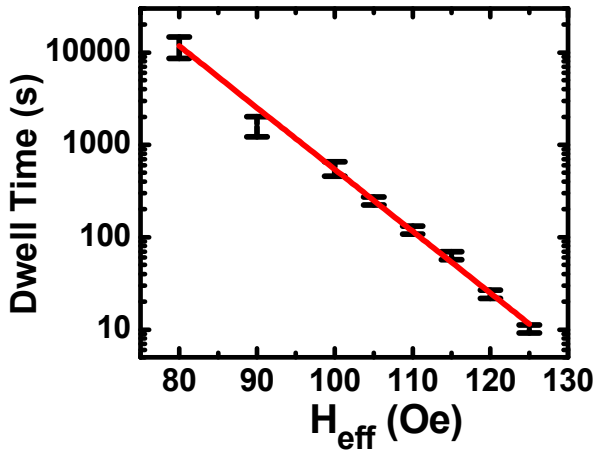

Fig. 9 The time required for thermally activated switching increases as H_{eff} is reduced. Extrapolation to H_{eff} = 0 yields an energy barrier of ~42kT (retention time > 50 years), confirming the thermal stability of our VMTJs.

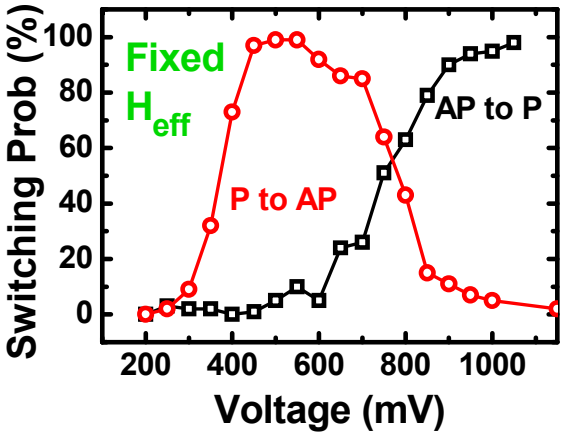

Fig. 10 Measured switching probability (based on 100 attempts with 100 ms long pulses) as a function of pulse voltage in a combined VCMA + STT device. Note that as in the case of Fig. 7, the same polarity of voltage is used for switching in both directions, while the pulse amplitude allows for controlling the switching direction without the need for varying external magnetic fields.

through the VMTJ, still not sufficient to bring about purely STT-induced switching, which contributes to a field-like STT acting as a voltage-dependent H_{eff} on the free layer. Therefore, the leakage current replaces the small effective magnetic field required in the VCMA-driven process.

In Figure 10 we demonstrate experimentally that VCMA and STT can be combined into a unipolar set/reset write scheme, where voltage pulses of the same polarity, but different amplitudes, are used to switch the device in opposite directions without changing H_{eff} (no external magnetic fields required) in the free layer. Voltage pulses of the opposite polarity will not switch the device (they will increase the coercivity of the free layer) thus they could be used to create disturb-free read schemes for the nonvolatile memory elements.

References

(1) R. Dorrance, F. Ren, Y. Toriyama, A. A. Hafez, C.-K. K. Yang, and D. Markovic, "Scalability and Design-Space Analysis of a 1T-1MTJ Memory Cell for STT-RAMs," *IEEE Trans. Electron Devices*, vol. 59, no. 4, pp. 878-887, April 2012

(2) T. Maruyama, et al., "Large voltage-induced magnetic anisotropy change in a few atomic layers of iron," *Nature Nanotechnology*, vol. 4, pp. 158-161, Mar 2009.

(3) J. Zhu, et al., "Voltage-Induced Ferromagnetic Resonance in Magnetic Tunnel Junctions," *Physical Review Letters*, vol. 108, p. 197203, 2012.

(4) J.G. Alzate, et al., "Voltage-Induced Switching of CoFeB-MgO Magnetic Tunnel Junctions," *in 56th Conference on Magnetism and Magnetic Materials,* Scottsdale, Arizona, 2011, pp. EG-11.

(5) W.-G. Wang, M. Li, S. Hageman and C.L. Chien, "Electric-field-assisted switching in magnetic tunnel junctions," *Nature Materials*, vol. 11, pp. 64-68, 2012.

(6) Y. Shiota, T. Nozaki, F. Bonell, S. Murakami, T. Shinjo and Y. Suzuki, "Induction of coherent magnetization switching in a few atomic layers of FeCo using voltage pulses," *Nature Materials*, vol. 11, pp. 39-43, 2012.

(7) P.K. Amiri, et al., "Switching current reduction using perpendicular anisotropy in CoFeB-MgO magnetic tunnel junctions," *Applied Physics Letters*, vol. 98, Mar 14 2011.